


 Available online at www.sciencedirect.com
SciVerse ScienceDirect

Nuclear Physics A 910–911 (2013) 478–481


www.elsevier.com/locate/nuclphysa

Measurement of isolated-photon+jet correlations in PbPb collisions at $\sqrt{s_{NN}} = 2.76$ TeV with CMS

Yue Shi Lai, for the CMS Collaboration

Abstract

A measurement of the transverse momentum balance in isolated-photon+jet pairs in PbPb collisions is described. The analysis is performed using a dataset recorded by the CMS experiment at the LHC from PbPb collisions at $\sqrt{s_{NN}} = 2.76$ TeV, corresponding to an integrated luminosity of $\int \mathcal{L} dt = 150 \mu\text{b}^{-1}$. For events containing an isolated photon with $p_T^\gamma > 60$ GeV/c and an associated jet with $p_T^{\text{jet}} > 30$ GeV/c, the photon+jet transverse momentum balance is studied as a function of collision centrality and compared to pp data and PYTHIA calculations. Using the isolated photon as the probe of the partonic energy at production, this measurement allows an unbiased characterization of the in-medium parton energy loss. With increasing collision centrality, a significant decrease in the ratio $p_T^{\text{jet}}/p_T^\gamma$ relative to the pp reference is observed.

1. Introduction

Enhanced production of highly asymmetric high transverse momentum (p_T) dijets has been observed by the ATLAS and CMS experiments in relativistic collisions of heavy nuclei [1, 2, 3]. While dijets are produced with a large yield, both jets undergo energy loss when transiting the medium, and therefore lose the kinematic information of the hard scattering. We present the first measurement of isolated-photon+jet momentum imbalance in $\sqrt{s_{NN}} = 2.76$ TeV pp and PbPb collisions with the CMS detector [6]. Photon production at leading order is back-to-back with the associated jet, and then escapes the medium without strong interaction. This allows us to observe differentially the kinematic information immediately at the hard scattering, and after the jet underwent medium interaction and hadronization [4, 5]. Experimentally, photon production with enriched prompt photon content is selected by an isolation requirement of the additional energy surrounding the direction of the photon.

2. Triggering, Photon and Jet Reconstruction

The data presented here consists of the PbPb data with an integrated luminosity of $\int \mathcal{L} dt = 150 \mu\text{b}^{-1}$, and a pp reference data set of $\int \mathcal{L} dt = 231 \text{nb}^{-1}$. Both data sets have been collected using the level-1 trigger with a $p_T > 5$ GeV/c threshold, and then by a subsequent high level trigger, that requires a reconstructed photon with $p_T > 40$ GeV/c in PbPb, and $p_T > 15$ GeV/c for pp.

Photon candidates with $p_T^\gamma > 60$ GeV/c are reconstructed from clusters deposited in the barrel part of the CMS electromagnetic calorimeter (ECAL) [6], which is limited to the pseudorapidity range of $|\eta^\gamma| < 1.44$. The clustering

Email address: ylai@mit.edu (Yue Shi Lai, for the CMS Collaboration)

© CERN for the benefit of the CMS Collaboration. Open access under [CC BY-NC-ND license](https://creativecommons.org/licenses/by-nc-nd/4.0/).

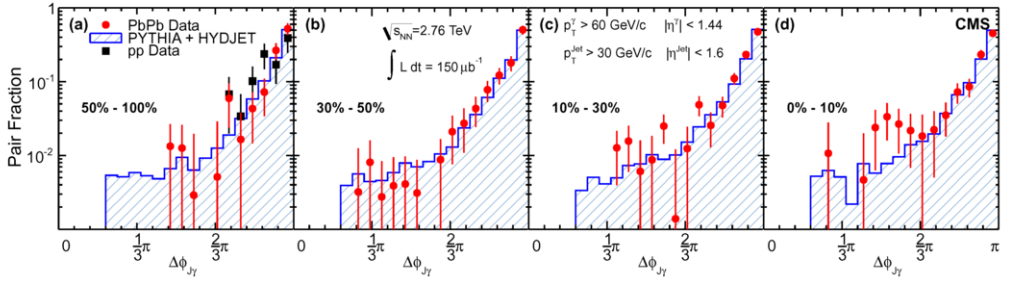


Figure 1: Azimuthal correlation $\Delta\phi_{J\gamma}$ between the photon and associated jet after background subtraction. The integral of each distribution is normalized to unity. All panels show PbPb data (filled circles) compared to the PYTHIA+HYDJET MC simulation (shaded histogram) in bins of increasing centrality from (a) to (d). The peripheral 50–100% PbPb data in (a) is also compared to pp data at $\sqrt{s} = 2.76$ TeV (filled squares). All error bars indicate the statistical uncertainty.

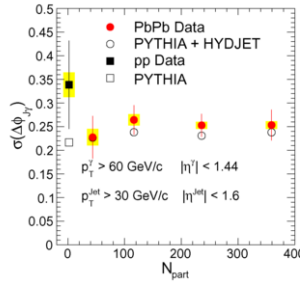


Figure 2: Fitted $\Delta\phi_{J\gamma}$ width (σ in Eq. (1)) between the photon and associated jet after background subtraction as a function of N_{part} . The fit range was restricted to $\Delta\phi_{J\gamma} > \frac{2}{3}\pi$. The error bars show the statistical uncertainty, while the yellow boxes indicate the point-to-point systematic uncertainties.

algorithm and rejection of heavily-ionizing particle interacting with the Si avalanche photodiodes is taken from [7]. Photon candidates coinciding with electron tracks are removed within $|\eta^\gamma - \eta^{\text{Track}}| < 0.02$ and $|\phi^\gamma - \phi^{\text{Track}}| < 0.15$. The effect of the PbPb underlying event (UE) on the reconstructed photon energy is corrected. An initial rejection of photons clearly coming from neutral meson decays is performed by requiring the ratio of hadronic to electromagnetic energy, $H/E < 0.1$, where the energy is summed within $\Delta R = \sqrt{\Delta\eta^2 + \Delta\phi^2} = 0.15$ around the photon candidate [8].

Photon isolation is provided by the sum of the track, hadronic calorimeter (HCAL), and ECAL energy within a $\Delta R < 0.4$. The UE contribution subtracted isolation variable $\text{SumIso}^{\text{UE-sub}}$ is constructed by removing the expectation value for the sum energy inside ΔR , determined by averaging over the η range that correspond to the pseudorapidity range of the ΔR cone and the full azimuth (excluding $\Delta R < 0.4$). To maintain high purity under the UE fluctuation, an increased cut of $\text{SumIso}^{\text{UE-sub}} < 1$ GeV is used, compared to $\text{SumIso}^{\text{UE-sub}} < 5$ GeV in [7].

Photon purities in each centrality interval are estimated using a two component, template fit of the shape of the electromagnetic shower in the ECAL, defined as a modified second moment, $\sigma_{\eta\eta}$, of the electromagnetic energy cluster distribution around its mean η position. The signal is required to have $\sigma_{\eta\eta} < 0.01$. The remaining contribution to the isolated-photon signal from decay of short-lived mesons is removed statistically using the purity estimated from the $\sigma_{\eta\eta}$ signal distribution. The $\sigma_{\eta\eta}$ signal distribution is obtained from PYTHIA+HYDJET simulation, while the background distribution is determined data-driven from the background enriched set of candidates with $10 < \text{SumIso}^{\text{UE-sub}} < 20$ GeV. The determined photon purity values from different centralities are 74–83%.

Jets are reconstructed from the particle-flow event reconstruction [9], and using the anti- k_T algorithm [10] with a distance parameter of $R = 0.3$. The UE energy is subtracted by the method in [11]. Jets with the isolated photon as a constituent are removed before correlating with themselves. Then all jets in the event, with $p_T^{\text{jet}} > 30$ GeV/c

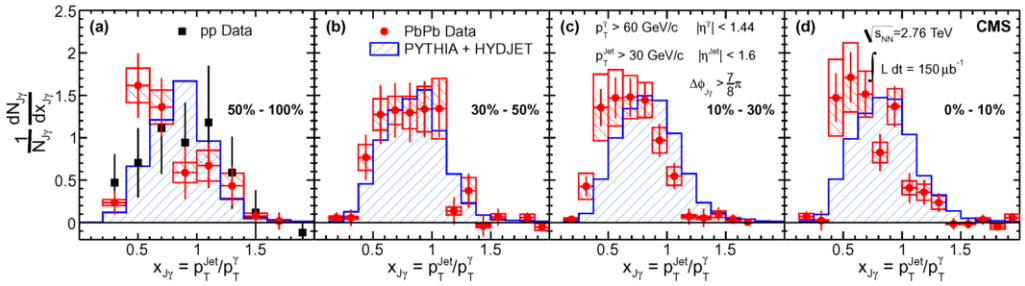


Figure 3: Distribution of the ratio between the photon ($p_T^\gamma > 60$ GeV/c) and jet ($p_T^{\text{jet}} > 30$ GeV/c, $\Delta\phi_{J\gamma} > \frac{7}{8}\pi$) momenta after subtracting background. The area of each distribution is normalized to unity. All panels show PbPb data (filled circles) to the PYTHIA+HYDJET MC simulation (shaded histogram) in bins of increasing centrality from (a) to (d). The peripheral 50–100% PbPb data in (a) is also compared to pp data at $\sqrt{s} = 2.76$ TeV (filled squares). The error bars on the points represent the statistical uncertainty. See text for an explanation of the open and shaded red systematic uncertainty boxes.

and within $|\eta^{\text{jet}}| < 1.6$ are correlated with the leading isolated photon in the event. Correlation with inclusive jets facilitates the statistical subtraction of the fake jets and multiple parton interactions contributing to the jet signal. These contributions are removed by event mixing and statistical subtraction. Direct rejection of fake jets using a fake jet discriminant has been used for cross check, although not used for the final result.

3. Monte Carlo Comparison

In addition to comparing the $\sqrt{s_{NN}} = 2.76$ TeV PbPb data with the pp data at the same \sqrt{s} , the data is also compared to PYTHIA version 6.422 [12], tune Z2, embedded into the PbPb background events generated by HYDJET [13] version 1.8 that is tuned to the multiplicity, single particle spectra, and elliptic flow observed in the LHC PbPb data. In order to check the subtraction procedure, we compared the momentum imbalance derived from the generator-level (without UE) particles with the high purity GenIso < 5 GeV isolation requirement to that obtained from the PYTHIA+HYDJET sample, filtered through the CMS full simulation, with the SumIso^{UE-sub} < 1 GeV condition. The difference is quoted as a systematic uncertainty.

To study the effect of potentially medium-modified jet fragmentation, the entire analysis procedure, which includes the particle flow event reconstruction and the subsequent jet reconstruction, has been additionally cross checked using PYQUEN [13] events embedded into HYDJET. The magnitude of the modification is observed to be comparable to our PbPb data, even though the N_{part} evolution is different. The full analysis procedure is found to properly extract the modified generator-level momentum imbalance.

4. Results

We study the possible medium effect on the azimuthal correlation between the photon and the jet using the unity-normalized $\Delta\phi_{J\gamma}$ distribution. To characterize the width of the $\Delta\phi_{J\gamma}$ distribution, we fit it against the unity-normalized, empirical parametrization

$$\frac{1}{N_{J\gamma}} \frac{dN_{J\gamma}}{d\Delta\phi_{J\gamma}} = \frac{e^{(\Delta\phi - \pi)/\sigma}}{(1 - e^{-\pi/\sigma})\sigma}, \quad (1)$$

and show the N_{part} dependence of the width parameter σ . Fig. 1 shows the $\Delta\phi_{J\gamma}$ distribution, where the PbPb data in each centrality bin is compared to the PYTHIA+HYDJET simulation. Additionally, the peripheral 50–100% centrality bin is also compared to the pp data at the same \sqrt{s} . Fig. 2 shows the width σ as a function of N_{part} . Both figures show that no significant change is observed between all PbPb centralities, the pp data, and PYTHIA tune Z2.

We study the effect of jet energy loss using the ratio of the jet p_T^{jet} by the photon p_T^γ , $x_{J\gamma} = p_T^{\text{jet}}/p_T^\gamma$. Fig. 3 shows the unity-normalized $x_{J\gamma}$ distribution, where the PbPb data in each centrality bin is compared to the PYTHIA+HYDJET simulation. Also here, the peripheral 50–100% centrality bin is compared to the pp data at the same \sqrt{s} . Due to the

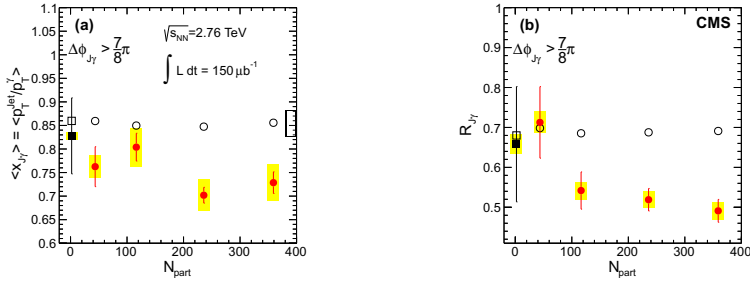


Figure 4: (a) Average ratio of jet transverse momentum to photon transverse momentum, $\langle x_{J\gamma} \rangle$, as a function of N_{part} . The empty box at the far right indicates the correlated systematic uncertainty. (b) Average fraction of isolated photons with an associated jet above 30 GeV/c, $R_{J\gamma}$, as a function of N_{part} . In both panels, the yellow boxes indicate point-to-point systematic uncertainties and the error bars denote the statistical uncertainty.

point-to-point anticorrelation, caused by the normalization, the probability density at low x must be balanced by a decrease at high x , so the points will move together towards the open (or shaded) areas of the systematic uncertainty boxes. Fig. 4(a) shows the corresponding N_{part} evolution of the distribution mean, $\langle x_{J\gamma} \rangle$. We observe a modest change in the $\langle x_{J\gamma} \rangle$ with increasing centrality, where the difference between PbPb and $\sqrt{s_{NN}} = 2.76$ TeV pp data is marginal, due to the large statistical uncertainty associated with the weak $\sqrt{s} = 2.76$ TeV pp statistics.

The second reason for the modest $\langle x_{J\gamma} \rangle$ evolution with centrality is due to the fact that $\langle x_{J\gamma} \rangle$ only describe the momentum imbalance of jets that still satisfying the kinematic cut. We therefore use the complementary variable of the fraction of photons with an associated jet, $R_{J\gamma}$, to show the migration of jets outside the kinematic window. Fig. 4(b) shows $R_{J\gamma}$ as a function of N_{part} . We observe a significant decrease of associated jets in central PbPb. We observe that the η distribution of PbPb jets is largely unchanged from pp, therefore the primary contribution to a decreased $R_{J\gamma}$ is the decreased jet p_T below the 30 GeV/c cut.

References

- [1] S. Chatrchyan, et al., Observation and studies of jet quenching in PbPb collisions at $\sqrt{s_{NN}} = 2.76$ TeV, Phys. Rev. C 84 (2011) 024906. arXiv:1102.1957, doi:10.1103/PhysRevC.84.024906.
- [2] G. Aad, et al., Observation of a centrality-dependent dijet asymmetry in lead-lead collisions at $\sqrt{s_{NN}} = 2.76$ TeV with the ATLAS detector at the LHC, Phys. Rev. Lett. 105 (2010) 252303. arXiv:1011.6182, doi:10.1103/PhysRevLett.105.252303.
- [3] S. Chatrchyan, et al., Jet momentum dependence of jet quenching in PbPb collisions at $\sqrt{s_{NN}} = 2.76$ TeV Submitted to Phys. Lett. B. arXiv:1202.5022.
- [4] X.-N. Wang, Z. Huang, I. Sarcevic, Jet quenching in the direction opposite to a tagged photon in high-energy heavy-ion collisions, Phys. Rev. Lett. 77 (1996) 231. arXiv:9701227, doi:10.1103/PhysRevLett.77.231.
- [5] X.-N. Wang, Z. Huang, Medium-induced parton energy loss in γ -jet events of high-energy heavy-ion collisions, Phys. Rev. C 55 (1997) 3047. arXiv:9605213, doi:10.1103/PhysRevC.55.3047.
- [6] S. Chatrchyan, et al., The CMS experiment at the CERN LHC, JINST 03 (2008) S08004. doi:10.1088/1748-0221/3/08/S08004.
- [7] S. Chatrchyan, et al., Measurement of isolated photon production in pp and PbPb collisions at $\sqrt{s_{NN}} = 2.76$ TeV, Phys. Lett. B 710 (2012) 256. doi:10.1016/j.physletb.2012.02.077.
- [8] V. Khachatryan, et al., Measurement of the isolated prompt photon production cross section in pp collisions at $\sqrt{s} = 7$ TeV, Phys. Rev. Lett. 106 (2011) 082001. arXiv:1012.0799, doi:10.1103/PhysRevLett.106.082001.
- [9] CMS Collaboration, Commissioning of the particle-flow reconstruction in minimum-bias and jet events from pp collisions at 7 TeV, CMS Physics Analysis Summary CMS-PAS-PFT-10-002 (2010).
- [10] M. Cacciari, G. P. Salam, G. Soyez, The anti- k_t jet clustering algorithm, JHEP 04 (2008) 063. arXiv:0802.1189, doi:10.1088/1126-6708/2008/04/063.
- [11] O. Kodolova, I. Vardanian, A. Nikitenko, A. Oulianov, The performance of the jet identification and reconstruction in heavy ions collisions with CMS detector, Eur. Phys. J. C 50 (2007) 117. doi:10.1140/epjc/s10052-007-0223-9.
- [12] T. Sjöstrand, S. Mrenna, P. Z. Skands, PYTHIA 6.4 physics and manual, JHEP 05 (2006) 026. arXiv:hep-ph/0603175, doi:10.1088/1126-6708/2006/05/026.
- [13] I. P. Lokhtin, A. M. Snigirev, A model of jet quenching in ultrarelativistic heavy ion collisions and high- p_T hadron spectra at RHIC, Eur. Phys. J. C 45 (2006) 211. arXiv:hep-ph/0506189, doi:10.1140/epjc/s2005-02426-3.